

# Analytical solution of transient heat conduction in a two-layer anisotropic cylindrical slab excited superficially by a short laser pulse

N.D. Milošević<sup>a,\*</sup>, M. Raynaud<sup>b</sup>

<sup>a</sup> *Laboratory for Thermal Engineering and Energy, Institute of Nuclear Sciences “Vinča”, P.O. Box 522, 11001 Belgrade, Serbia and Montenegro*

<sup>b</sup> *Institut National des Sciences Appliquées de Lyon, CETHIL, UMR CNRS 5008, 20 Av. A. Einstein, 69621 Villeurbanne Cedex, France*

Received 13 March 2003; received in revised form 31 October 2003

## Abstract

This paper presents an exact analytical solution of 2D transient temperature, caused by a non-periodical pulse heating of a cylindrical two-layer slab. The corresponding partial differential equations are solved step-by-step, using the separation of variables technique. Analytical/computational procedure for eigenvalue derivation is considered separately. General initial assumptions, such as existence of thermal contact resistance, thermal conduction and diffusion anisotropy, radiative heat losses, non-uniform heating, and finite absorption depth are accounted in the solution. Numerical simulations of temperature distribution throughout the sample are given at the end of the paper.

© 2003 Elsevier Ltd. All rights reserved.

*Keywords:* Anisotropic materials; Pulse heating; Two-dimensional heat conduction; Two-layer structures

## 1. Introduction

Composite, multi-layered, anisotropic, reinforced, and generally all kind of structured materials have found numerous applications in engineering and science in the last decades. Two and three-dimensional heat conduction in such materials are one of the most important physical phenomena needed to be theoretically or experimentally considered. In that sense, there are numerous contributions available in scientific journals and books.

Regarding the theory, analytical mono-dimensional heat conduction throughout a multi-layer system, described by simple Cartesian or cylindrical geometry, is

studied very often in detail, comprising different boundary and initial conditions. However, there are no many published examples treating multi-dimensional heat conduction in such a system. Salt [1,2] made a comprehensive study of two-dimensional transient heat conduction in composites in the Cartesian coordinate system, but neglecting thermal contact resistance and supposing the isotropy of layers. Similar problem of three-dimensional transient conduction in composite slab is treated by Mikhailov and Özişik [3] with particular attention to the computational procedure of eigenvalues earlier proposed by Mikhailov and Vulchanov [4]. Yan et al. [5] published theoretical research of the same problem but with thin film acting as a heat source. Recently, Aviles-Ramos et al. [6] offered an exact transient solution for the case of rectangular shaped partially isotropic composite. In cylindrical coordinate system Abdul Azeed and Vakakis [7] applied double integral transformation to obtain the solution of two-dimensional semi-infinite composite media, but supposing the perfect contact between layers and thermal isotropy.

\* Corresponding author. Tel.: +381-11-24-40-871; fax: +381-11-24-53-670.

E-mail address: [nenadm@rt270.vin.bg.ac.yu](mailto:nenadm@rt270.vin.bg.ac.yu) (N.D. Milošević).

### Nomenclature

$a$	thickness of the first layer
$A, B, C, D$	coefficients
$b$	thickness of the second layer
$c$	specific heat
$d$	sample radius
$d_f$	radius of heated region
$f$	function whose zeros are eigenvalues
$h$	axial heat transfer coefficient
$h_r$	radial heat transfer coefficient
$k_{\perp}, k_{\parallel}$	normal- and parallel-to-sample-plane thermal conductivity
$K$	ratio between parallel- and normal-to-sample-plane thermal conductivity
$Q$	pulse heating energy, absorbed by sample, per square meter
$r$	radial coordinate
$R_c$	thermal contact resistance
$s, N, P$	solution functions

$t$	time
$T$	transient temperature
$x$	axial coordinate

### Greek symbols

$\alpha_{\perp}, \alpha_{\parallel}$	normal- and parallel-to-sample-plane thermal diffusivity
$\beta, \lambda$	independent eigenvalues
$\varepsilon$	absorption depth
$\varphi$	spatial distribution of absorbed pulse energy
$\Phi$	radial component of transient temperature
$\gamma, \eta$	dependent eigenvalues
$\Gamma$	temporal component of transient temperature
$\Theta$	temporal pulse function
$\rho$	density of material
$\tau$	pulse heating duration
$\Psi$	axial component of transient temperature

General assumptions of materials' thermal anisotropy and finite contact resistance were taken by Cole and McGahan [8] as the extension of their previously published theory [9]. They studied in cylindrical coordinate system heat conduction in multi-layers excited by laser absorption and used integral Hankel transformation and Green's functions to solve particular boundary value problem that include the continuous heat generation.

This paper treats, using separation of variable technique, two-dimensional heat conduction in a composite slab heated discontinuously by a short laser pulse, comprising also the assumptions considered by Cole and McGahan [8]. Besides, the paper considers the influence of the laser pulse duration and offers two solutions: one supposing the instantaneous pulse and the other with the finite pulse time. Also, it presents the results derived from both general and also uniform distribution of absorbed pulse energy.

The reason of such analysis is to provide the analytical solution of a particular problem of 2D transient heat conduction through the small-sized media (thin films, for example) where the numerical solution, obtained by any of the most convenient numerical procedures, such as the alternate direction implicit (ADI) method or Crank–Nicholson procedure, may not be sufficiently reliable and exact. In comparison to the previous analytical solutions, this paper dealing with the simple separation of variable technique, supposes the most general boundary and initial conditions, which can be useful, for example, in heat conduction modeling or dynamical methods for thermophysical characterization of layered materials [10].

## 2. Statement of the problem

Let two-layer composite sample be in the cylindrical form, as presented on Fig. 1(a). The layers are from different materials, characterized by proper thermo-physical properties, such as thermal conductivity,  $k$ , heat capacity,  $c$ , and density,  $\rho$ . In addition, let both materials be anisotropic regarding their thermal conductivities in such a way that one distinguishes  $k_{1\parallel}$  and  $k_{2\parallel}$  for parallel, and  $k_{1\perp}$  and  $k_{2\perp}$  for perpendicular direction to the sample plane. Assuming a non-ideal contact between the layers, one needs to consider, also, the finite thermal contact resistance,  $R_c$ .

Heat transfer through the sample could be mathematically described by the cylindrical coordinate system, as presented on Fig. 1(b), so that the contact between the layers and the sample center represent zero in both axial and also radial direction. Thickness of first and second layer is  $a$  and  $b$ , and sample radius is  $d$ . Axial and radial heat transfer coefficients  $h_1, h_2, h_{r1}$ , and  $h_{r2}$ , describe linear boundary conditions of third kind between sample surfaces and environment. The temperature of the sample environment, as well as the sample initial temperature before the heating begins, are assumed to be zero.

Let an initial radiant flux of duration  $\tau$  and spatial energy distribution described by a non-dimensional function  $\varphi(r)$  begin to impact at time  $t = 0$  the front sample side on the centered circular surface of radius  $d_f$ , as shown on Fig. 1(b). Let  $Q$  be a part of energy per square meter of the flux, absorbed in a very thin volume of thickness  $\varepsilon$  ( $\varepsilon \ll a$ ) and radius  $d_f$  of the first layer. The

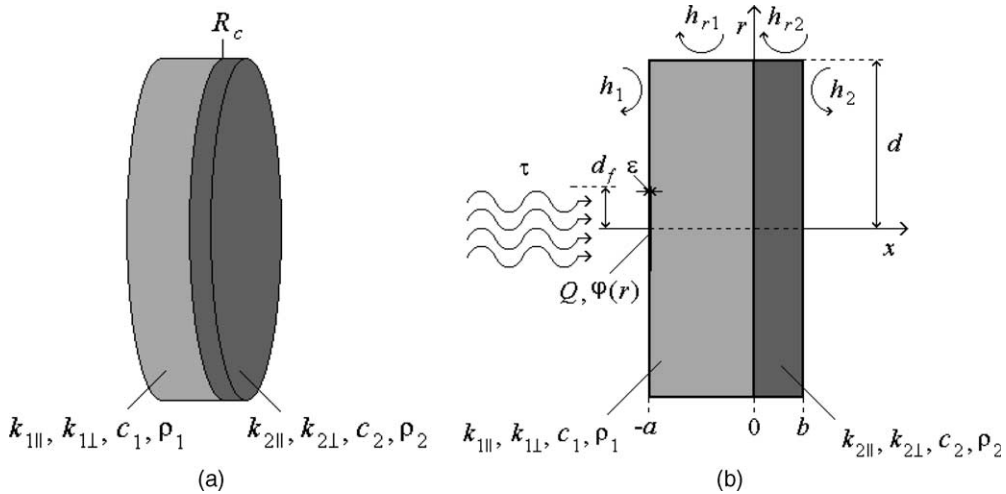


Fig. 1. (a) Two-layer composite sample; (b) Corresponding cylindrical coordinate system.

heat, thus generated, propagates throughout the sample by conduction, axially and radially, from front to back sample side and from center to periphery. If one assumes that there is no heat source and sink in the sample, thermophysical properties are independent on temperature (usually justified for small amplitudes of transient temperature), and, for instance, initial flux is infinitely short, i.e. having the form of Dirac pulse ( $\tau = 0$ ), one can set the system of linear partial differential equations as follows

$$k_{1\perp} \frac{\partial^2 T_1}{\partial x^2} + k_{1\parallel} \left( \frac{1}{r} \frac{\partial T_1}{\partial r} + \frac{\partial^2 T_1}{\partial r^2} \right) = \rho_1 c_1 \frac{\partial T_1}{\partial t}, \quad -a \leq x < 0, \quad 0 \leq r \leq d, \quad t > 0 \quad (1a)$$

$$k_{2\perp} \frac{\partial^2 T_2}{\partial x^2} + k_{2\parallel} \left( \frac{1}{r} \frac{\partial T_2}{\partial r} + \frac{\partial^2 T_2}{\partial r^2} \right) = \rho_2 c_2 \frac{\partial T_2}{\partial t}, \quad 0 < x \leq b, \quad 0 \leq r \leq d, \quad t > 0 \quad (1b)$$

with corresponding boundary and initial conditions

$$\frac{\partial T_1}{\partial x} = h_1 T_1, \quad x = -a, \quad t > 0 \quad (2a)$$

$$\frac{\partial T_2}{\partial x} = -h_2 T_2, \quad x = b, \quad t > 0 \quad (2b)$$

$$k_{1\perp} \frac{\partial T_1}{\partial x} = k_{2\perp} \frac{\partial T_2}{\partial x}, \quad x = 0, \quad t > 0 \quad (2c)$$

$$T_2 - T_1 = k_{1\perp} R_c \frac{\partial T_1}{\partial x}, \quad x = 0, \quad t > 0 \quad (2d)$$

$$k_{1\parallel} \frac{\partial T_1}{\partial r} = -h_{r1} T_1, \quad r = d, \quad t > 0 \quad (2e)$$

$$k_{2\parallel} \frac{\partial T_2}{\partial r} = -h_{r2} T_2, \quad r = d, \quad t > 0 \quad (2f)$$

$$T_1 = \begin{cases} \frac{Q}{\rho_1 c_1 \varepsilon} \varphi(r), & -a \leq x \leq -a + \varepsilon, \quad 0 \leq r \leq d_f, \quad \varepsilon \ll a \\ 0, & -a + \varepsilon \leq x \leq 0, \quad 0 \leq r \leq d_f, \quad t = 0 \\ 0, & -a \leq x \leq 0, \quad d_f < r \leq d \end{cases} \quad (2g)$$

$$T_2 = 0, \quad t = 0 \quad (2h)$$

### 3. Analytical solution

The problem stated in Eqs. (1) and (2) can be resolved by the separation of variables method, but with one restriction: boundary conditions of the lateral sample surfaces (2e) and (2f) must be of first or second kind. It means that radial heat transfer coefficients must be equal to zero ( $h_{r1} = h_{r2} = 0$ ), i.e. heat flux over the lateral sample surface (adiabatic conditions), or the temperature of lateral surfaces must be set to zero. The same condition was taken in [5] for a rectangular-shaped sample. The reason of such assumption will be discussed later in this section.

Supposing that the temperature  $T$  represent a product of three functions, each depending of either one space or one time variable,

$$T(x, r, t) = \Psi(x)\Phi(r)\Gamma(t) \quad (3)$$

the partial differential Eqs. (1) can be, therefore, rewritten as

$$\frac{1}{\Psi_1} \frac{\partial^2 \Psi_1}{\partial x^2} + K_1 \frac{1}{\Phi_1} \left( \frac{1}{r} \frac{\partial \Phi_1}{\partial r} + \frac{\partial^2 \Phi_1}{\partial r^2} \right) - \frac{1}{\alpha_{1\perp}} \frac{1}{\Gamma_1} \frac{\partial \Gamma_1}{\partial t} = 0 \quad (4a)$$

$$\frac{1}{\Psi_2} \frac{\partial^2 \Psi_2}{\partial x^2} + K_2 \frac{1}{\Phi_2} \left( \frac{1}{r} \frac{\partial \Phi_2}{\partial r} + \frac{\partial^2 \Phi_2}{\partial r^2} \right) - \frac{1}{\alpha_{2\perp}} \frac{1}{\Gamma_2} \frac{\partial \Gamma_2}{\partial t} = 0 \tag{4b}$$

where  $\alpha_{\perp} = k_{\perp}/(\rho c)$  is thermal diffusivity in perpendicular direction and  $K = k_{\parallel}/k_{\perp}$ . Eq. (4) hold only if each addend is equal to a constant, independent of any space or time variable, i.e. when

$$\frac{1}{\Gamma_1} \frac{\partial \Gamma_1}{\partial t} = \frac{1}{\Gamma_2} \frac{\partial \Gamma_2}{\partial t} \equiv -\beta^2 \tag{5}$$

$$\frac{1}{\Phi_1} \left( \frac{1}{r} \frac{\partial \Phi_1}{\partial r} + \frac{\partial^2 \Phi_1}{\partial r^2} \right) = \frac{1}{\Phi_2} \left( \frac{1}{r} \frac{\partial \Phi_2}{\partial r} + \frac{\partial^2 \Phi_2}{\partial r^2} \right) \equiv -\lambda^2 \tag{6}$$

and consequently

$$\frac{1}{\Psi_1} \frac{\partial^2 \Psi_1}{\partial x^2} = -\frac{\beta^2}{\alpha_{1\perp}} + K_1 \lambda^2 \equiv -\gamma^2 \tag{7a}$$

$$\frac{1}{\Psi_2} \frac{\partial^2 \Psi_2}{\partial x^2} = -\frac{\beta^2}{\alpha_{2\perp}} + K_2 \lambda^2 \equiv -\eta^2 \tag{7b}$$

New differential Eqs. ((5)–(7)) are to be solved separately considering corresponding boundary and initial conditions derived from Eqs. ((2a)–(2e), (2h)).

In order to obtain new or separated boundary and initial conditions, parameters  $h_{r1}$  and  $h_{r2}$  from (2e) and (2f) must be first set to zero, i.e. assume either adiabatic or invariant boundary conditions on both lateral sample surfaces. In opposite, the radial components of temperature  $\Phi_1$  and  $\Phi_2$  would always be different (except when  $k_{1\parallel} = k_{2\parallel}$  and  $h_{r1} = h_{r2}$ ) and the separation of the contact boundary condition in (2c) would not be possible. Separated boundary and initial conditions are then as follows:<sup>1</sup>

$$\frac{\partial \Psi_1}{\partial x} = h_1 \Psi_1, \quad x = -a, \quad t > 0 \tag{8a}$$

$$\frac{\partial \Psi_2}{\partial x} = -h_2 \Psi_2, \quad x = b, \quad t > 0 \tag{8b}$$

$$k_{1\perp} \frac{\partial \Psi_1}{\partial x} = k_{2\perp} \frac{\partial \Psi_2}{\partial x}, \quad x = 0, \quad t > 0 \tag{8c}$$

$$\Psi_2 - \Psi_1 = k_{1\perp} R_c \frac{\partial \Psi_1}{\partial x}, \quad x = 0, \quad t > 0 \tag{8d}$$

$$\frac{\partial \Phi_1}{\partial r} = \frac{\partial \Phi_2}{\partial r} = 0, \quad r = d, \quad t > 0 \tag{8e}$$

$$\Psi_1 = \begin{cases} \frac{Q}{\rho_1 c_1 \varepsilon}, & -a \leq x \leq -a + \varepsilon, \quad \varepsilon \ll a \\ 0, & -a + \varepsilon \leq x \leq 0 \end{cases} \quad t = 0 \tag{8f}$$

$$\Psi_2 = 0, \quad t = 0 \tag{8g}$$

$$\Phi_1 = \begin{cases} \varphi(r), & 0 \leq r \leq d_f \\ 0, & d_f < r \leq d \end{cases} \quad t = 0 \tag{8h}$$

$$\Phi_2 = 0, \quad t = 0 \tag{8i}$$

From (6) and (7), one can see that the eigenvalues  $\lambda$  and  $\beta$  are independent, while those  $\gamma$  and  $\eta$  depends on the first two. In other words, for each eigenvalue  $\lambda_i$  ( $i = 1, 2, \dots$ ) and  $\beta_n$  ( $n = 1, 2, \dots$ ), one needs to calculate  $\gamma_{n,i}$  and  $\eta_{n,i}$ .

The complete sample temperature is equal to summation of solutions for each independent eigenvalue  $\lambda$  and  $\beta$ , or

$$T(x, r, t) = \sum_{i=1}^{+\infty} \sum_{n=1}^{+\infty} P_{n,i} \Psi_{n,i}(x) \Phi_i(r) \Gamma_n(t) \tag{9}$$

where the coefficients  $P_{n,i}$  are derived from the property of eigenfunctions orthogonality and depend on the initial conditions.

The general solutions of Eqs. ((5)–(7)) are, respectively,

$$\Gamma_{1n} = \Gamma_{2n} = e^{-\beta_n^2 t} \tag{10}$$

$$\Phi_{1i} = \Phi_{2i} = J_0(\lambda_i r) \tag{11}$$

and

$$\Psi_{1n,i} = A \sin(\gamma_{n,i} x) + B \cos(\gamma_{n,i} x) \tag{12a}$$

$$\Psi_{2n,i} = C \sin(\eta_{n,i} x) + D \cos(\eta_{n,i} x) \tag{12b}$$

Eigenvalues  $\lambda_i$  ( $i = 1, 2, \dots$ ) represent positive roots of the transcendental equation obtained from (11) applying the boundary condition (8e):

$$\lambda_i J_1(\lambda_i d) = 0 \tag{13}$$

Solutions of Eq. (13) are obtainable by some numerical technique, for example by well-known Newton–Raphson method.<sup>2</sup> The first root,  $\lambda_1 = 0$ , is taken in consideration, as suggested in [11] for the case of adiabatic boundary condition using the cylindrical coordinate system.

Introducing the boundary conditions ((8a)–(8d)) in (12), one can derive a linear algebraic system over the coefficients  $A, B, C$ , and  $D$  as

<sup>1</sup> For the purpose of unity accordance in (3), radial and temporal components are dimensionless while the axial holds the unit Kelvin, as it stated in (8f) and (8h).

<sup>2</sup> The corresponding iteration formula is  $\frac{y_{k+1}^{(i)}}{y_k^{(i)}} = 1 - \frac{J_1(y_k^{(i)})}{y_k^{(i)} J_0(y_k^{(i)}) - J_1(y_k^{(i)})}$ , where  $y_k^{(i)} \equiv \lambda_i/d$  with  $y_0^{(i)}$  as an arbitrary chosen value.

$$\begin{bmatrix} s_{1n,i} & s_{2n,i} & 0 & 0 \\ 0 & 0 & s_{3n,i} & s_{4n,i} \\ k_{1\perp}\gamma_{n,i} & 0 & -k_{2\perp}\eta_{n,i} & 0 \\ k_{1\perp}R_c\gamma_{n,i} & 1 & 0 & -1 \end{bmatrix} \begin{bmatrix} A \\ B \\ C \\ D \end{bmatrix} = 0 \quad (14)$$

where

$$s_{1n,i} \equiv k_{1\perp}\gamma_{n,i} \cos(\gamma_{n,i}a) + h_1 \sin(\gamma_{n,i}a) \quad (15a)$$

$$s_{2n,i} \equiv k_{1\perp}\gamma_{n,i} \sin(\gamma_{n,i}a) - h_1 \cos(\gamma_{n,i}a) \quad (15b)$$

$$s_{3n,i} \equiv k_{2\perp}\eta_{n,i} \cos(\eta_{n,i}b) + h_2 \sin(\eta_{n,i}b) \quad (15c)$$

$$s_{4n,i} \equiv -k_{2\perp}\eta_{n,i} \sin(\eta_{n,i}b) + h_2 \cos(\eta_{n,i}b) \quad (15d)$$

If one expresses coefficients  $B$ ,  $C$ , and  $D$  as a function of  $A$ , like

$$B = -\frac{s_{1n,i}}{s_{2n,i}}A, \quad C = \frac{k_{1\perp}\gamma_{n,i}}{k_{2\perp}\eta_{n,i}}A, \quad (16)$$

$$D = -\frac{k_{1\perp}\gamma_{n,i}}{k_{2\perp}\eta_{n,i}}\frac{s_{3n,i}}{s_{4n,i}}A$$

the axial components of temperature from (12) become

$$\Psi_{1n,i} = A \left[ \sin(\gamma_{n,i}x) - \frac{s_{1n,i}}{s_{2n,i}} \cos(\gamma_{n,i}x) \right] \quad (17a)$$

$$\Psi_{2n,i} = A \frac{k_{1\perp}}{k_{2\perp}} \frac{\gamma_{n,i}}{\eta_{n,i}} \left[ \sin(\eta_{n,i}x) - \frac{s_{3n,i}}{s_{4n,i}} \cos(\eta_{n,i}x) \right] \quad (17b)$$

On the other hand, in order to avoid the trivial solution of linear system in (14), the determinant of the square matrix must be zero for each eigenvalue  $\lambda_i$  and  $\beta_n$ , or

$$f_{n,i} = k_{2\perp}\eta_{n,i}s_{1n,i}s_{4n,i} - k_{1\perp}\gamma_{n,i}s_{2n,i}s_{3n,i} - k_{1\perp}k_{2\perp}R_c\gamma_{n,i}\eta_{n,i}s_{2n,i}s_{4n,i} \equiv 0 \quad (18)$$

It means that the eigenvalues  $\beta_n$  represent the roots of the function  $f_i$  over the variable  $\beta$ , for given  $\lambda_i$ . The function  $f_i$  can be solved when two unknowns,  $\gamma_{n,i}$  and  $\eta_{n,i}$ , are changed with  $\gamma_{n,i} = (\beta_n^2/\alpha_{1\perp} - K_1\lambda_i^2)^{1/2}$  and  $\eta_{n,i} = (\beta_n^2/\alpha_{2\perp} - K_2\lambda_i^2)^{1/2}$ , using (7). The solutions of  $f_i$  give, therefore, the eigenvalues  $\beta_n$ , say  $\beta_n^{(i)}$  for each eigenvalue  $\lambda_i$ . Nevertheless, only those positive and bigger than zero are taken for the final solution of temperature.

Function  $f_i$  in (18) depends on  $\beta$  very awkwardly for each  $\lambda_i$ . For example, supposing the parameter values from Section 4, the function  $f_i$  is presented on Fig. 2 for  $\lambda_1 = 0$ , and on Fig. 3 for  $\lambda_2 > 0$ . One can see that, for  $\lambda_1 = 0$ , the function  $f_i$  is real in the whole domain of positive values  $\beta$ , while its imaginary part appears when  $\lambda > 0$ . Then, there are, in fact, two different imaginary functions, limited by zero,  $\beta_{\gamma=0}^{(i)}$ , and  $\beta_{\eta=0}^{(i)}$  (c.f. Fig. 3). The latter two values are derived from

$$\beta_{\gamma=0}^{(i)} = \lambda_i \sqrt{\alpha_{1\perp}K_1}, \quad \beta_{\eta=0}^{(i)} = \lambda_i \sqrt{\alpha_{2\perp}K_2} \quad (19)$$

When  $\beta_n^{(i)} < \min[\beta_{\gamma=0}^{(i)}, \beta_{\eta=0}^{(i)}]$ , both of  $\gamma_{n,i}$  and  $\eta_{n,i}$  are complex and the function  $f_i$  becomes imaginary, too. For

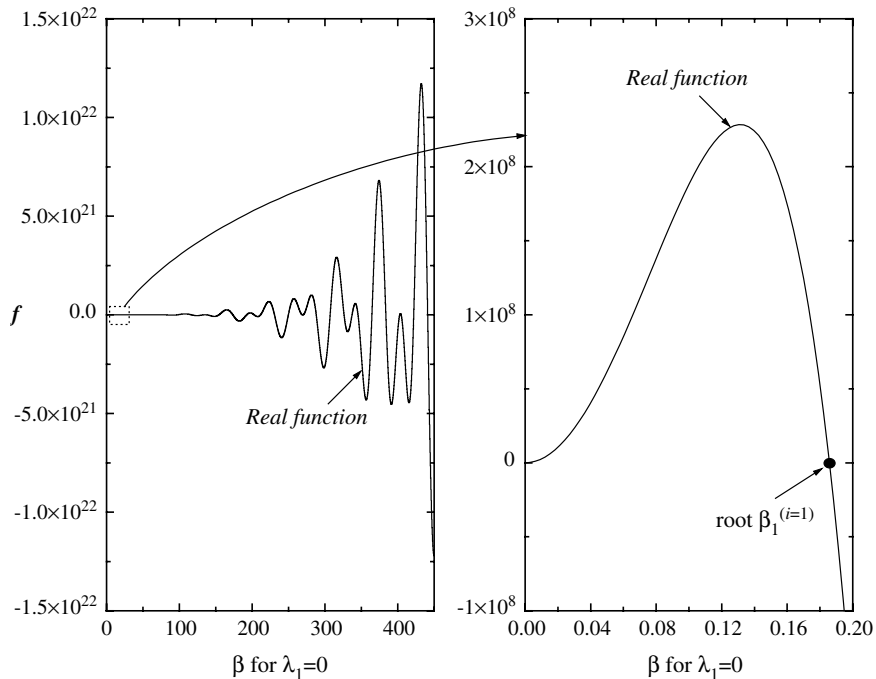


Fig. 2. Function  $f$  whose roots represent eigenvalues  $\beta_n^{(i=1)}$  for  $\lambda_1 = 0$ .

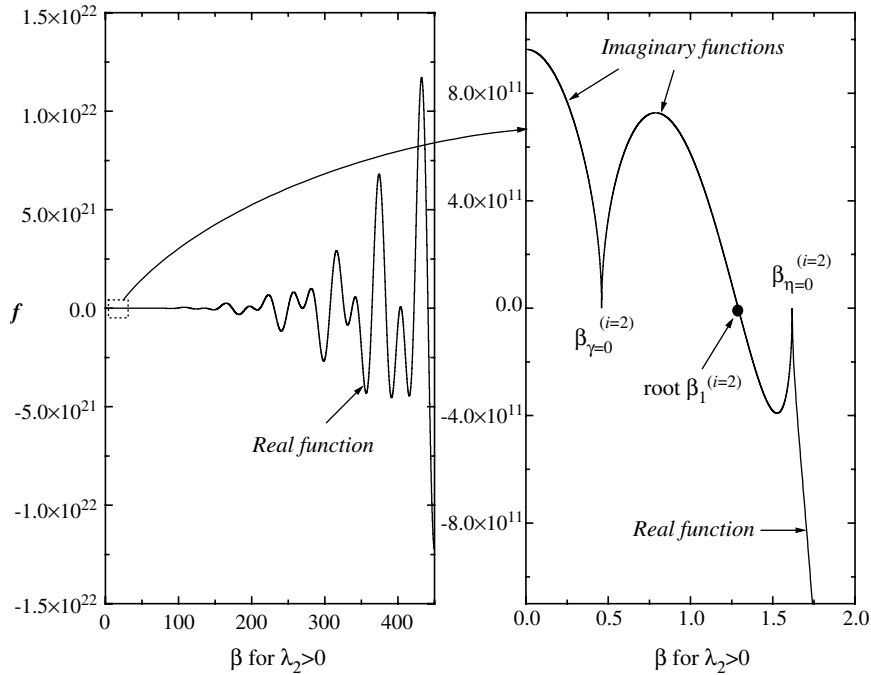


Fig. 3. Function  $f$  whose roots represent eigenvalues  $\beta_n^{(i=2)}$  for  $\lambda_2 > 0$ .

$\min[\beta_{\gamma=0}^{(i)}, \beta_{\eta=0}^{(i)}] < \beta_n^{(i)} < \max[\beta_{\gamma=0}^{(i)}, \beta_{\eta=0}^{(i)}]$  one of coefficients  $\gamma_{n,i}$  and  $\eta_{n,i}$  is imaginary and the function  $f_i$  gets the second imaginary form (Fig. 3). It can be proved easily that there are no roots in the first imaginary form when both  $\gamma_{n,i}$  and  $\eta_{n,i}$  are complex. In the second form however, there is, at least, one eigenvalue  $\beta_n^{(i)}$  and it rises gradually with  $i$ . Regarding the real part of the function  $f_i$ , it always comprises the infinite number of eigenvalues.

Generally, from Figs. 2 and 3 one can easily notice the fast alternation and very high amplitudes of the function  $f_i$ , which means very high function derivative. This fact normally offers good possibilities for numerical solution of function's roots. Using the Newton–Raphson method for example, results can be obtained very fast, but with one condition: it is necessary to have all corresponding initial values, near to those of true eigenvalues. However, just this last requirement makes the resolution of (18) still difficult.

Taking the same parametric values as above, the first 20 calculated roots  $\beta_n^{(i)}$  for  $\lambda_i$  from  $i = 1$  to  $i = 200$  are presented<sup>3</sup> on Fig. 4. Apparently, the distribution of eigenvalues is quasi-regular, but hardly predictable for small values of  $i$ .

There is another technique for determination of the roots  $\beta_n^{(i)}$ , which avoids the resolution of (18). Mikhailov and Vulchanov [4] proposed a method for general forms

of Sturm–Liouville problems, and for particular problem of transient conduction in multi-dimensional composite region [3]. This technique, named “sign-count”, provides the automatic computation of eigenvalues, and guarantees, as stated, the highest precision and error-free results.

As it is said above, coefficients  $P_{n,i}$  in (9) can be derived from the characteristic of orthogonality of the eigenfunctions in (11) and (17), and from the initial conditions in (8f), (8g), (8h), and (8i). Namely, if one develops, using (9), the initial radial and axial component  $\Phi_1(t = 0) \equiv \varphi(r)$ ,  $\Psi_{1n,i}(t = 0) \equiv F_1$ , and  $\Psi_{2n,i}(t = 0) \equiv F_2$ , multiplies them with  $rJ_0(\lambda_j r)$  and  $\Psi_{1m,i}$ , i.e. with  $rJ_0(\lambda_j r)$  and  $\Psi_{2m,i}$ , integrates from 0 to  $d$  over  $r$ , from  $-a$  to 0, and from 0 to  $b$  over  $x$ , and makes an addition of these two (single, for each layer) equations, one gets finally

$$\begin{aligned} & \rho_1 c_1 \int_0^d \int_{-a}^0 r \varphi(r) J_0(\lambda_j r) F_1 \Psi_{1m,i} dr dx \\ & + \rho_2 c_2 \int_0^d \int_0^b r \varphi(r) J_0(\lambda_j r) F_2 \Psi_{2m,i} dr dx \\ & = \rho_1 c_1 \sum_{i=1}^{+\infty} \sum_{n=1}^{+\infty} P_{n,i} \int_0^d \int_{-a}^0 r J_0(\lambda_i r) J_0(\lambda_j r) \Psi_{1n,i} \Psi_{1m,i} dr dx \\ & + \rho_1 c_1 \sum_{i=1}^{+\infty} \sum_{n=1}^{+\infty} P_{n,i} \int_0^d \int_0^b r J_0(\lambda_i r) J_0(\lambda_j r) \Psi_{2n,i} \Psi_{2m,i} dr dx \end{aligned} \tag{20}$$

where parameters  $\rho_1 c_1$  and  $\rho_2 c_2$  are so-called discontinuous weight factors for multi-layered region, intro-

<sup>3</sup> Every third  $i$  value is presented on Fig. 4.

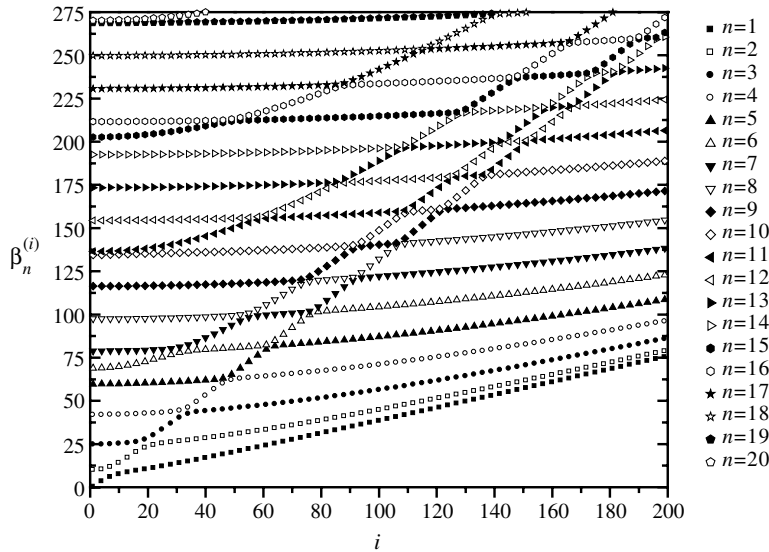


Fig. 4. Eigenvalues  $\beta_n^{(i)}$  ( $n = 1, 2, \dots, 20$ ) for each  $\lambda_i$  ( $i = 1, 2, \dots, 200$ ).

duced by Tittle [12]. Due to the orthogonality, products  $J_0(\lambda_i r)J_0(\lambda_j r)$ ,  $\Psi_{1m,i}\Psi_{1n,i}$ , and  $\Psi_{2m,i}\Psi_{2n,i}$  are different from zero only for  $i = j$  and  $m = n$ , so (20) reduces to

$$P_{n,i} = \frac{2}{d^2 J_0^2(\lambda_i d)} \int_0^d r \varphi(r) J_0(\lambda_i r) dr \times \frac{1}{N_{n,i}} \left( \rho_1 c_1 \int_{-a}^0 F_1 \Psi_{1n,i} dx + \rho_2 c_2 \int_0^b F_2 \Psi_{2n,i} dx \right) \tag{21}$$

where

$$N_{n,i} = \rho_1 c_1 \int_{-a}^0 \Psi_{1n,i}^2 dx + \rho_2 c_2 \int_0^b \Psi_{2n,i}^2 dx \tag{22}$$

Solving the integrals in (22) and using some trigonometrical identities, the function  $N_{n,i}$  is equal to

$$N_{n,i} = A^2 \frac{\rho_1 c_1}{4 \gamma_{n,i}} \left\{ 2 \frac{s_{1n,i}}{s_{2n,i}} [1 - \cos(2\gamma_{n,i} a)] + \sin(2\gamma_{n,i} a) \left( \frac{s_{1n,i}^2}{s_{2n,i}^2} - 1 \right) + 2\gamma_{n,i} a \left( \frac{s_{1n,i}^2}{s_{2n,i}^2} + 1 \right) \right\} + A^2 \rho_2 c_2 \frac{k_{1\perp}^2}{k_{2\perp}^2} \frac{\gamma_{n,i}^2}{4 \eta_{n,i}^3} \left\{ 2 \frac{s_{3n,i}}{s_{4n,i}} [\cos(2\eta_{n,i} b) - 1] + \sin(2\eta_{n,i} b) \left( \frac{s_{3n,i}^2}{s_{4n,i}^2} - 1 \right) + 2\eta_{n,i} b \left( \frac{s_{3n,i}^2}{s_{4n,i}^2} + 1 \right) \right\} \tag{23}$$

Knowing the functions  $F_1$  and  $F_2$  from the initial conditions (8f) and (8g), the coefficients  $P_{n,i}$  become

$$P_{n,i} = -4A \frac{Q}{d^2 \varepsilon} \int_0^{d_f} r \varphi(r) J_0(\lambda_i r) dr \frac{1}{J_0^2(\lambda_i d)} \frac{1}{N_{n,i} \gamma_{n,i}} \times \left[ \sin \frac{\gamma_{n,i}(2a - \varepsilon)}{2} \sin_{n,i} \frac{\gamma_{n,i} \varepsilon}{2} + \frac{s_{1n,i}}{s_{2n,i}} \cos \frac{\gamma_{n,i}(2a - \varepsilon)}{2} \sin \frac{\gamma_{n,i} \varepsilon}{2} \right] \tag{24}$$

If one assumes that the absorption depth of pulse energy is much smaller than the thickness of the first layer ( $\varepsilon \ll a$  or  $\varepsilon \rightarrow 0$ ),<sup>4</sup> Eq. (24) takes a simpler form

$$\lim_{\varepsilon \rightarrow 0} P_{n,i} = -2A \frac{Q}{d^2} \frac{1}{J_0^2(\lambda_i d)} \frac{1}{N_{n,i}} \int_0^{d_f} r \varphi(r) J_0(\lambda_i r) dr \times \left[ \sin(\gamma_{n,i} a) + \frac{s_{1n,i}}{s_{2n,i}} \cos(\gamma_{n,i} a) \right] \tag{25}$$

According to (9,10,11), (17), and (25), the sample temperature in the case of instantaneous incident pulse ( $\tau = 0$ ) becomes

$$T_1(x, r, t, \tau = 0) = 2 \frac{Q}{d^2} \sum_{i=1}^{+\infty} \frac{J_0(\lambda_i r)}{J_0^2(\lambda_i r)} \int_0^{d_f} r \varphi(r) J_0(\lambda_i r) dr \times \sum_{n=1}^{+\infty} \frac{1}{N_{n,i}} \left[ \sin(\gamma_{n,i} a) + \frac{s_{1n,i}}{s_{2n,i}} \cos(\gamma_{n,i} a) \right] \times \left[ -\sin(\gamma_{n,i} x) + \frac{s_{1n,i}}{s_{2n,i}} \cos(\gamma_{n,i} x) \right] e^{-\beta_{n,i}^2 t} \tag{26a}$$

<sup>4</sup> This can be assumed for opaque solid materials.

$$\begin{aligned}
 T_2(x, r, t, \tau = 0) &= 2 \frac{Q}{d^2} \frac{k_{1\perp}}{k_{2\perp}} \sum_{i=1}^{+\infty} \frac{J_0(\lambda_i r)}{J_0^2(\lambda_i d)} \int_0^{d_f} r \varphi(r) J_0(\lambda_i r) dr \\
 &\times \sum_{n=1}^{+\infty} \frac{1}{\bar{N}_{n,i}} \frac{\gamma_{n,i}}{\eta_{n,i}} \left[ \sin(\gamma_{n,i} a) + \frac{s_{1n,i}}{s_{2n,i}} \cos(\gamma_{n,i} a) \right] \\
 &\times \left[ -\sin(\eta_{n,i} x) + \frac{s_{3n,i}}{s_{4n,i}} \cos(\eta_{n,i} x) \right] e^{-\beta_{n,i}^2 t}
 \end{aligned} \tag{26b}$$

where the function  $\bar{N}_{n,i}$  is given by (23), but without the parameter  $A$ .

Numerical evaluation of temperatures  $T_1$  and  $T_2$  from (26) could be relatively long for some parameters of the model, what depends primarily on the computation time of eigenvalues  $\beta_n^{(i)}$  from (18), whose total number should satisfy the acceptable convergence of the expressions (26). For example, very short transient temperature times generally require great number of  $\beta_n^{(i)}$  for each eigenvalue  $\lambda_i$ . A detailed analysis of eigenvalues and their behavior in a multi-layered slab, using the Cartesian coordinates and implying certain physical conditions, are given by Salt [2].

### 3.1. The case of uniform heating

For practical evaluation of temperatures from (26) one must have the non-dimensional function  $\varphi(r)$ . Its simplest form is unity,  $\varphi(r) \equiv 1$ , which represents the uniform distribution of absorbed pulse energy or the uniform sample heating. In reality, such heating can be assumed under certain experimental conditions.

Setting  $\varphi(r) \equiv 1$ , the coefficients  $P_{n,i}$  from (24) become

$$\begin{aligned}
 P_{n,i} &= -4A \frac{Q d_f}{d^2 \varepsilon} \frac{J_1(\lambda_i d_f)}{\lambda_i J_0^2(\lambda_i d)} \frac{1}{N_{n,i} \gamma_{n,i}} \left[ \sin \frac{\gamma_{n,i}(2a - \varepsilon)}{2} \sin \frac{\gamma_{n,i} \varepsilon}{2} \right. \\
 &\left. + \frac{s_{1n,i}}{s_{2n,i}} \cos \frac{\gamma_{n,i}(2a - \varepsilon)}{2} \sin \frac{\gamma_{n,i} \varepsilon}{2} \right]
 \end{aligned} \tag{27}$$

or when  $\varepsilon \ll a$  or  $\varepsilon \rightarrow 0$

$$\begin{aligned}
 \lim_{\varepsilon \rightarrow 0} P_{n,i} &= -2A \frac{Q d_f}{d^2} \frac{J_1(\lambda_i d_f)}{\lambda_i J_0^2(\lambda_i d)} \frac{1}{N_{n,i}} \\
 &\times \left[ \sin(\gamma_{n,i} a) + \frac{s_{1n,i}}{s_{2n,i}} \cos(\gamma_{n,i} a) \right]
 \end{aligned} \tag{28}$$

Before writing the final form of temperature in the case of the uniform heating, the problem of the first root,  $\lambda_1 = 0$ , should be considered, because if one applies  $\lambda_1$  in (27) or (28), the term 0/0 will appear. However, if one develops Bessel function of the first order, the expression  $J_1(z)/z$  tends to 1/2 when  $z \rightarrow 0$ , and the indefinite term will disappear. As a result, assuming the instantaneous uniform heating, the sample temperatures finally become

$$\begin{aligned}
 T_1(x, r, t, \tau = 0) &= Q \frac{d_f^2}{d^2} \left[ 1 + \frac{2}{d_f} \sum_{i=2}^{+\infty} \frac{J_1(\lambda_i d_f)}{\lambda_i J_0^2(\lambda_i d)} J_0(\lambda_i r) \right] \\
 &\times \sum_{n=1}^{+\infty} \frac{1}{\bar{N}_{n,i}} \left[ \sin(\gamma_{n,i} a) + \frac{s_{1n,i}}{s_{2n,i}} \cos(\gamma_{n,i} a) \right] \\
 &\times \left[ -\sin(\gamma_{n,i} x) + \frac{s_{1n,i}}{s_{2n,i}} \cos(\gamma_{n,i} x) \right] e^{-\beta_{n,i}^2 t}
 \end{aligned} \tag{29a}$$

$$\begin{aligned}
 T_2(x, r, t, \tau = 0) &= Q \frac{k_{1\perp}}{k_{2\perp}} \frac{d_f^2}{d^2} \left[ 1 + \frac{2}{d_f} \sum_{i=2}^{+\infty} \frac{J_1(\lambda_i d_f)}{\lambda_i J_0^2(\lambda_i d)} J_0(\lambda_i r) \right] \\
 &\times \sum_{n=1}^{+\infty} \frac{1}{\bar{N}_{n,i}} \frac{\gamma_{n,i}}{\eta_{n,i}} \left[ \sin(\gamma_{n,i} a) + \frac{s_{1n,i}}{s_{2n,i}} \cos(\gamma_{n,i} a) \right] \\
 &\times \left[ -\sin(\eta_{n,i} x) + \frac{s_{3n,i}}{s_{4n,i}} \cos(\eta_{n,i} x) \right] e^{-\beta_{n,i}^2 t}
 \end{aligned} \tag{29b}$$

where the function  $\bar{N}_{n,i}$  is given by (23), without the coefficient  $A$ . Multiplying the unity inside the first brackets of (29a) and (29b) with the series over the index  $n$ , the value  $i = 1$  is implied.

### 3.2. The case of extended heating

If the initial flux has the finite duration  $\tau$ , the solution can be obtained using either the theorem of Duhamel [13], applied on the expressions given by (26) or (29), or the technique of superposition, proposed by Watt [14], for the purpose of the laser flash method.<sup>5</sup> According to the latter, the temperature of sample, being the result of finite pulse heating described by a temporal function  $\Theta(t, \tau)$ , is given by

$$T(x, r, t, \tau > 0) = \frac{\int_0^t \Theta(t', \tau) T(x, r, t - t', \tau = 0) dt'}{\int_0^\tau \Theta(t', \tau) dt'} \tag{30}$$

for  $t > \tau$ . For  $t \leq \tau$  the same expression is valid, but with parameter  $t$  instead of  $\tau$  for the upper limits of both integrals [14]. Having (9), Eq. (30) reduces to

$$T(x, r, t, \tau > 0) = \sum_{i=1}^{+\infty} \sum_{n=1}^{+\infty} P_{n,i} \Psi_{n,i} \Phi_i \Gamma_{n,i}^* \tag{31}$$

where

$$\Gamma_{n,i}^* = \frac{\int_0^t \Theta(t', \tau) e^{-\beta_{n,i}^2(t-t')} dt'}{\int_0^\tau \Theta(t', \tau) dt'} \tag{32}$$

<sup>5</sup> This method is standard technique for thermal diffusivity measurements.

The function  $\Theta(t, \tau)$  represents the evolution of pulse energy and, in practice, it is usually approximated with some standard theoretical form, such as rectangular, triangular, or exponential one. For example, if the laser radiative energy is approximated by the simplest rectangular form

$$\Theta(t, \tau) = \begin{cases} 1, & 0 \leq t \leq \tau \\ 0, & t > \tau \end{cases} \quad (33)$$

the function  $\Gamma_{n,i}^*$  becomes

$$\Gamma_{n,i}^* = \begin{cases} \frac{1}{\beta_{n,i}^2} (1 - e^{-\beta_{n,i}^2 t}), & 0 < t \leq \tau \\ \frac{1}{\beta_{n,i}^2} (e^{\beta_{n,i}^2 \tau} - 1) e^{-\beta_{n,i}^2 t}, & t > \tau \end{cases} \quad (34)$$

#### 4. Numerical examples of transient temperature response

Theoretical temperature responses are computed using the expressions for uniform instantaneous (Eqs. (29), and extended (Eq. (30)) pulse heating, where the pulse energy is absorbed superficially ( $\varepsilon \rightarrow 0$ ). The spatial and temporal evolution of sample temperature is presented on one type of multi-layered sample in the form of two equally thick layers, but from two different materials. Copper as good and titan as bad heat conductor were chosen for layers' materials. Only for demonstration purpose, perpendicular and parallel components of thermal diffusivities were kept equal. The sample had the form of coin, small in thickness and large in diameter. Constant parameters were  $a = b = 0.5$  mm,  $d = 25.4$  mm,  $d_f = 5$  mm,  $\alpha_{1\perp} = \alpha_{1\parallel} = 9.3 \times 10^{-6}$  m<sup>2</sup> s<sup>-1</sup>,  $\alpha_{2\perp} = \alpha_{2\parallel} = 1.15 \times 10^{-4}$  m<sup>2</sup> s<sup>-1</sup>,  $\rho_1 = 4500$  kg m<sup>-3</sup>,  $\rho_2 = 8930$  kg m<sup>-3</sup>,  $c_1 = 522$  J kg<sup>-1</sup> K<sup>-1</sup>,  $c_2 = 386$  J kg<sup>-1</sup> K<sup>-1</sup>,  $h_1 = 50$  W m<sup>-2</sup> K<sup>-1</sup>,  $h_2 = 50$  W m<sup>-2</sup> K<sup>-1</sup>, and  $Q = 100$  J m<sup>-2</sup>, while the values of thermal contact resistance  $R_c$  and pulse heating duration  $\tau$  were varied.

##### 4.1. Titan–copper sample with low contact resistance and instantaneous pulse heating

In this numerical simulation, the thermal contact resistance between the layers has been taken to be relatively low,  $R_c = 5 \times 10^{-6}$  m<sup>2</sup> K W<sup>-1</sup>, while the pulse heating duration infinitely short ( $\tau = 0$ ). Then, temperature distribution for a choice of moments after the pulse heating looks like as presented on Fig. 5. Just after the impact of incident flux, isothermal lines are located around the incident surface of the first layer (Fig. 5(a)). At the moment  $t = 5$  ms through the second layer, there is already a certain level of heat conduction, shown on the smaller diagram (the right-hand top side of Fig. 5(a)). However, such conduction is very weak, according to much smaller temperature gradient than in the first material. At  $t = 10$  ms (Fig. 5(b)), while the temperature

gradient in the first layer declines, in the second grows.<sup>6</sup> Isothermal lines begin to disperse into the sample axial direction due to the high copper conductivity (the right-hand top side of Fig. 5(b)). Later, at  $t = 50$  ms (Fig. 5(c)), heat in copper moves only in radial direction and begins to do the same in the titan layer. Temperature values fall in the first and increase in the second layer, simultaneously. Far later, at  $t = 500$  ms (Fig. 5(d)), there is no significant axial temperature distribution. After long time period, in 5 s (Fig. 5(e)), the temperature along and across the sample is practically uniform, but the redistribution of small temperature gradient still exists. Because front and back sample sides are under the influence of finite heat transfer coefficients  $h_1$  and  $h_2$ , transient temperature tends to zero with gradient directed to both basis surfaces. In 50 s (Fig. 5(f)), there is no temperature gradient across the sample, while the axial one is small, but greater than zero. The transient temperature over the sample is near to zero, being slightly higher in the second layer than in the first one, because of the lower heat capacity of copper.

This numerical simulation shows the logical sequences of heat diffusion. The heat begins to diffuse in both directions from impact surface to periphery and to the contact between the layers. It passes gradually to the second layer where the high thermal diffusivity of copper straightens the isothermal lines very fast. At one moment, the temperature gradient orientates oppositely and heat diffuses from copper to titan layer. Although thermal contact resistance exists between the layers, in this case it does not influence significantly the overall temperature gradient.

##### 4.2. Titan–copper sample with high contact resistance and instantaneous incident pulse

Having the same parametric values as in the previous example, but with thermal contact resistance two orders higher ( $R_c = 5 \times 10^{-4}$  m<sup>2</sup> K/W), the heat diffusion through the sample is much altered. In this case, the temperature distribution for different times after the pulse heating is presented on Fig. 6. In comparison to the example with low thermal contact resistance, heat propagates from titan to copper layer with a significant time delay. In 5 ms (Fig. 6(a)), copper received much less initial energy than in the first example. The same situation is in 10 ms. Titan cools slowly and the temperature

<sup>6</sup> In order to emphasize the variation of the temperature gradient rather than that of its absolute values, every frame has its own temperature scale, shown on the right side. Therefore, regardless the absolute temperature values, the temperature range is always presented by full gray scale, from color white (the highest temperatures) to color black (the lowest temperatures).

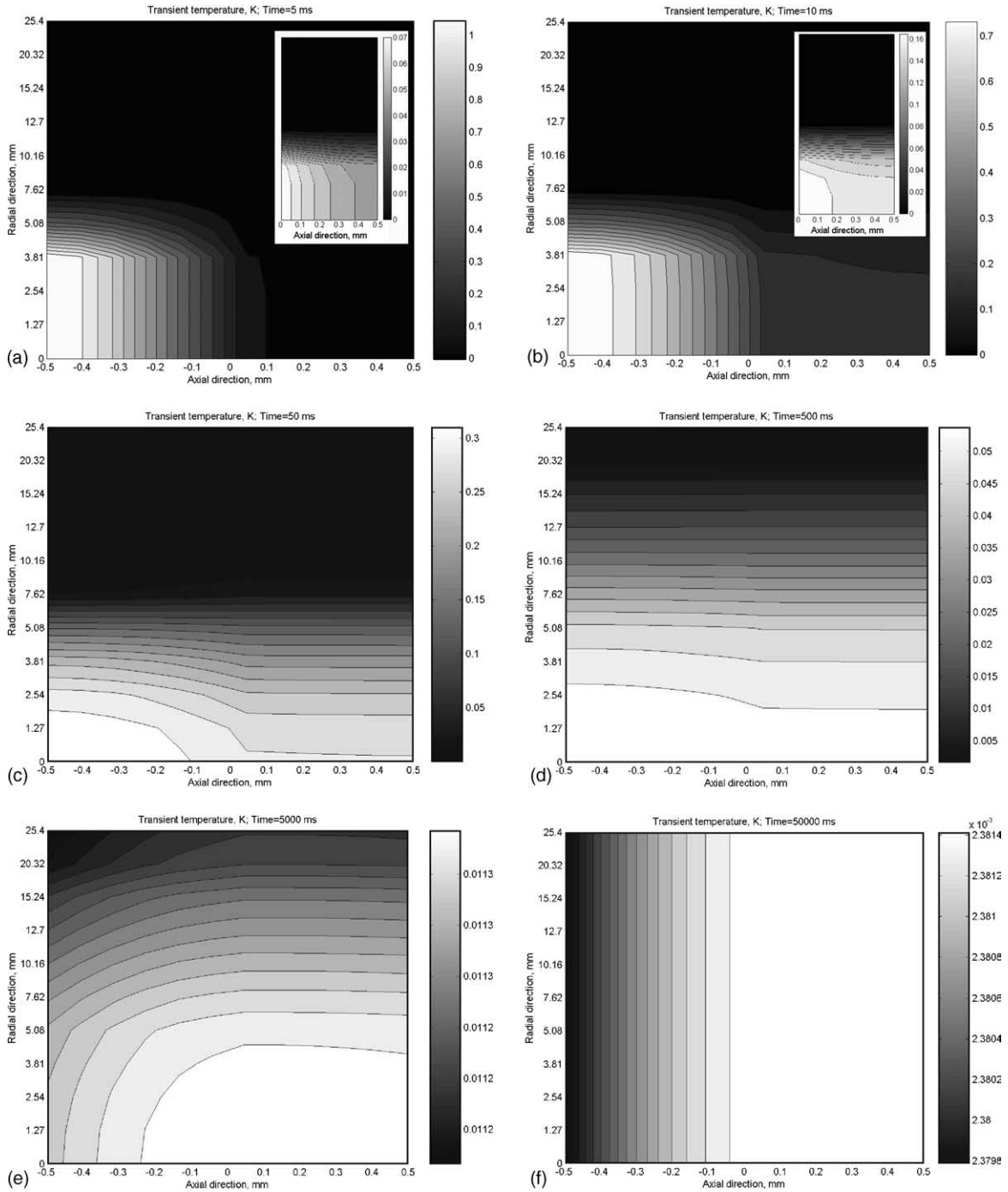


Fig. 5. Temperature distribution in the case of titan–copper sample with low thermal contact resistance and instantaneous incident pulse.

gradient is almost directed radially over there. After 50 ms (Fig. 6(c)), the temperature of titan is still much higher than that in the copper layer, although both

gradients are orientated radially. Situation is not much changed in 0.5 s, too. At 5 s, the sample temperature becomes almost equal, but with still existing gradient,

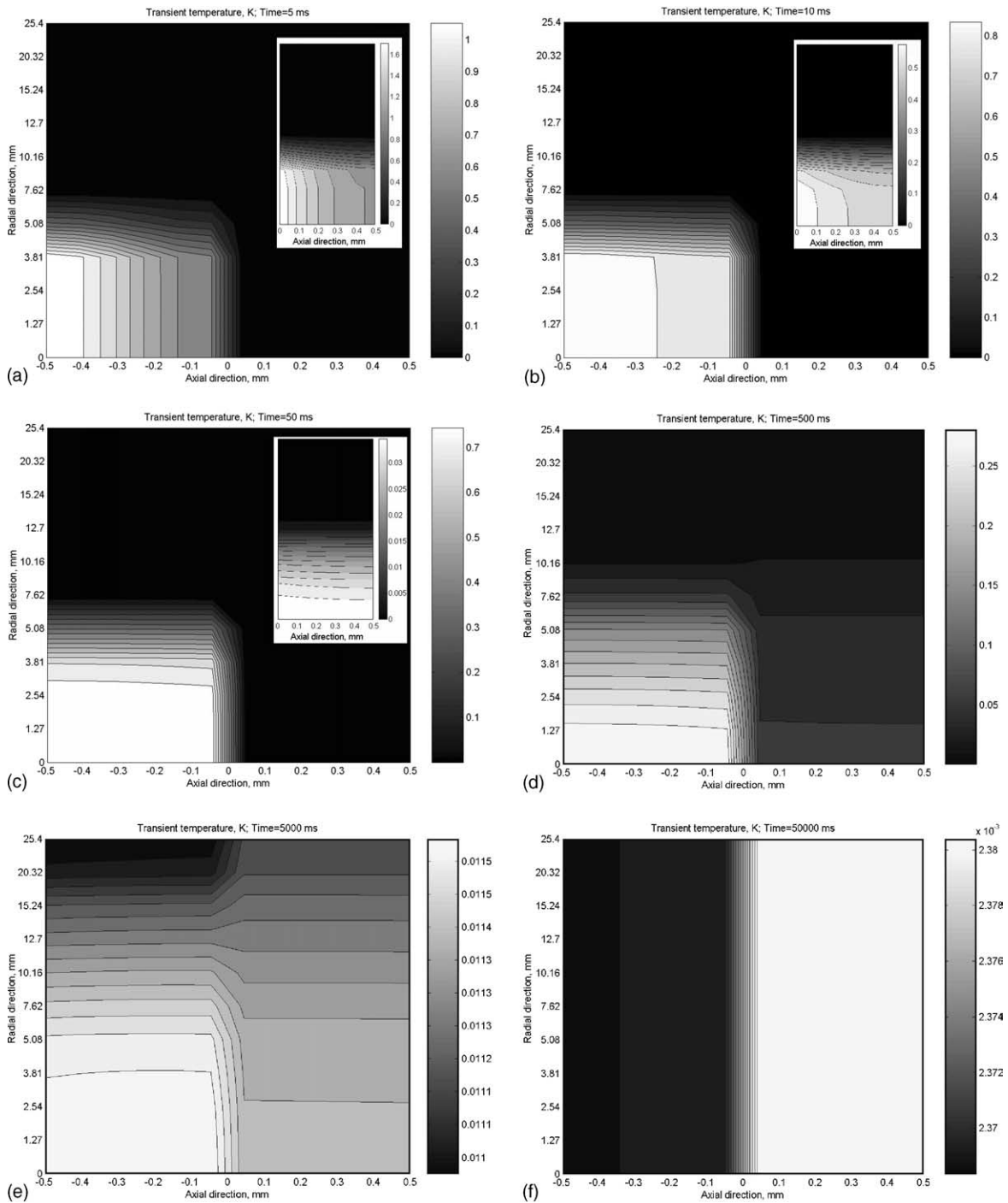


Fig. 6. Temperature distribution in the case of titan–copper sample with high thermal contact resistance and instantaneous incident pulse.

which begins to direct itself from copper toward titan layer. Finally, in  $t = 50$  s (Fig. 6(f)), the temperature distribution in this and previous example is practically same.

As expected, high value of thermal contact resistance has a strong effect on transient heat diffusion through the sample. Namely, it delays the continuous heat diffusion from first to second layer and vice versa.

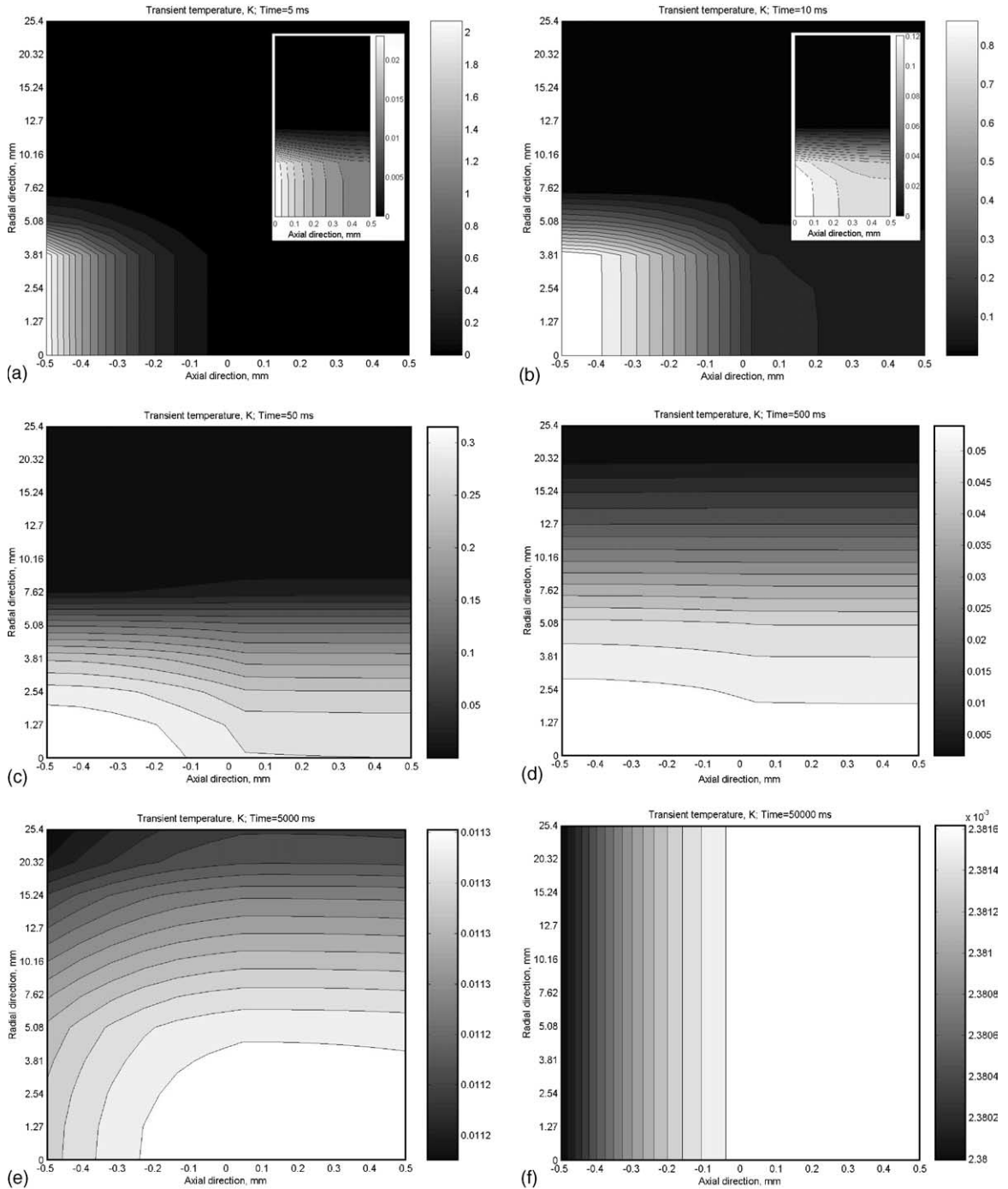


Fig. 7. Temperature distribution in the case of titan–copper sample with low thermal contact resistance and prolonged incident pulse.

4.3. Titan–copper sample with low contact resistance and finite incident pulse

This example is the same as the first one (Section 4.1), unless the pulse heating has finite duration greater than

zero, i.e.  $\tau > 0$ . The logical consequence is that the temperature gradient and temperature values are higher, at the same transient time, than those in the case of instantaneous incident pulse. Numerical simulation of this case is presented on Fig. 7. For  $t = 5$  ms (Fig. 7(a)),

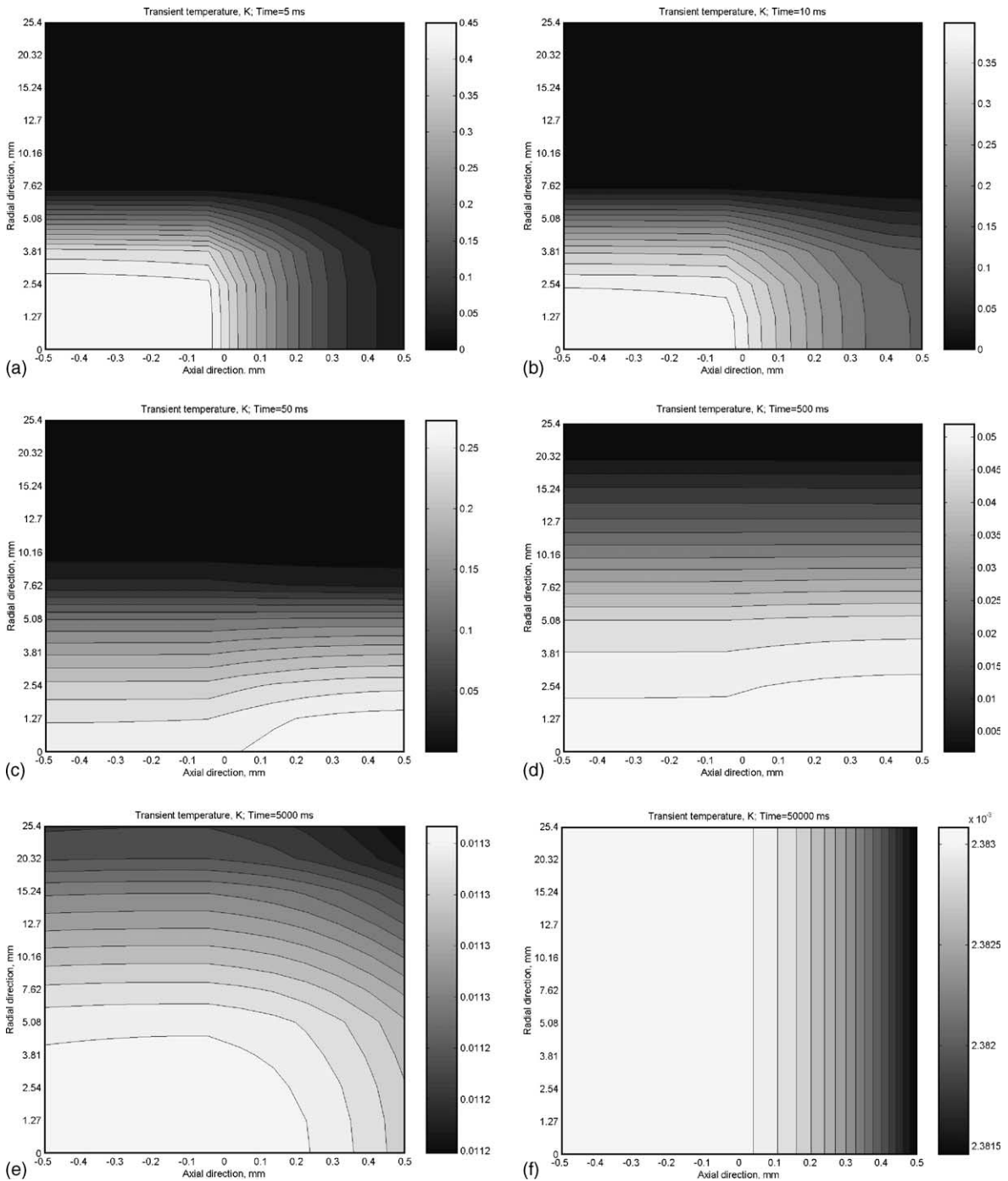


Fig. 8. Temperature distribution in the case of copper–titan sample with low thermal contact resistance and instantaneous incident pulse.

just about the end of heating ( $\tau = 5$  ms), absolute values of transient temperature and its gradient are higher than in the first example (c.f. Fig. 5(a)) and concentrated mostly around the incident surface. Nevertheless, such

differences are obvious only in a short post-pulse period. At  $t = 50$  ms, for example, temperature and its gradient are similar to those in the first case, and subsequently they will practically be the same.

Therefore, this numerical example shows that the finite pulse heating affects the heat diffusion only in the period during and shortly after the sample heating takes place. It is implied that the duration of incident pulse does not generate the sample overheating, where the problem becomes non-linear.

#### 4.4. Copper–titan sample with low contact resistance and instantaneous incident pulse

This example operates with the same parameters as the first one, but with the inverse order of layer materials. The copper layer, therefore, absorbs the initial pulse energy, and the titan layer receives the heat over the contact with copper. Because copper is much better conductor than titan, overall heat transfer through the sample cannot be symmetric in the first period after the heating.

The distribution of transient temperature is presented on Fig. 8 for this case. Soon after the heating, at  $t = 5$  ms (Fig. 8(a)), isothermal lines in copper turn axially, so that the temperature gradient exists for the most part only in radial direction. At the same time, heat advances already toward the second layer. At 10 ms (Fig. 8(b)), the heat begins to flow radially through the second layer, while at 50 ms (Fig. 8(c)), the temperature gradient in titan is mostly directed toward the periphery. In the same moment, however, the maximum of heat is concentrated around the sample center, on the back sample surface. From that region, the heat diffuses then reversely, toward the first layer. Following sequences are practically completely symmetric in comparison with those of the first example.

Therefore, the simple rotation of the sample, regarding the direction of pulse heating, changes temperature values and gradient only in the first transient period. When the heat passes through the contact and reaches the surface of the second layer, the rotation of sample layers has no practical effect on the temperature distribution, because the heat propagates symmetrically over the entire sample.

## 5. Conclusion

Two-dimensional transient heat conduction in two-layer composite slab in the case of short, non-uniform pulse heating can be analytically described by the separation of variable method, using cylindrical coordinate system. In order to resolve three systems for each space and time variable, one needs to have separated boundary and initial conditions. This can be achieved only by setting the lateral boundary conditions to be of either first or second order.

The solution of the transient temperature, being a function of model's parameters, represents a double

summation over two eigenvalues: one as the roots of Bessel function of the first order, and the other as the solution of a particular function that depends on both first eigenvalue and also model parameters. At least two numerical methods are available in the literature for the computation of both eigenvalues.

Characteristics, such as finite thermal contact resistance between the layers, cylindrical anisotropy of materials' thermal diffusivity or conductivity, and finite absorption depth can be readily included into the theoretical model. The effect of finite heating time can be considered separately, by the method of superposition.

Using the thermophysical properties of titan (bad conductor) and copper (good conductor), with low and high thermal contact resistance, and with instantaneous and extended pulse heating, the distribution of transient temperature over the sample for different time values after the heating is computed and presented for demonstration purpose. Numerical examples have shown that the heat diffuses in all directions, including the reverse one. The thermal contact resistance has the effect of "thermal barrage", which slows down the heat diffusion over the contact and forces the radial diffusion, while the finite heating time has the influence on temperature values and gradient during the period and after the heating.

With given analytical solution the transient temperature of two-layer sample could be completely described at any time, in any sample point, and for any set of parametric values. This information is important for design, optimization, and characterization of layered structures when a non-periodic pulse heating takes place.

## References

- [1] H. Salt, Transient conduction in a two-dimensional composite slab—I. Theoretical development of temperature modes, *Int. J. Heat Mass Transfer* 26 (1983) 1611–1616.
- [2] H. Salt, Transient conduction in a two-dimensional composite slab—II. Physical interpretation of temperature modes, *Int. J. Heat Mass Transfer* 26 (1983) 1617–1623.
- [3] M.D. Mikhailov, M.N. Özişik, Transient conduction in a three-dimensional composite slab, *Int. J. Heat Mass Transfer* 29 (1986) 340–342.
- [4] M.D. Mikhailov, N.L. Vulchanov, Computational procedure for Sturm–Liouville problems, *J. Comput. Phys.* 50 (1983) 323–336.
- [5] L. Yan, A. Haji-Sheikh, J.V. Beck, Thermal characteristics of two-layered bodies with embedded thin-film heat source, *ASME J. Electron. Packaging* 115 (1993) 276–283.
- [6] C. Aviles-Ramos, A. Haji-Sheikh, J.V. Beck, Exact solution of heat conduction in composite materials and application to inverse problems, *J. Heat Transfer—Trans. ASME* 120 (1998) 592–599.

- [7] M.F. Abdul Azeez, A.F. Vakakis, Axisymmetric transient solutions of the heat diffusion problem in layered composite media, *Int. J. Heat Mass Transfer* 43 (2000) 3883–3895.
- [8] K.D. Cole, W.A. McGahan, Theory of multilayers heated by laser absorption, *J. Heat Transfer—Trans. ASME* 115 (1993) 767–771.
- [9] W.A. McGahan, K.D. Cole, Solutions of the heat conduction equation in multilayers for photothermal deflection experiments, *J. Appl. Phys.* 72 (1992) 1362–1373.
- [10] N.D. Milošević, M. Raynaud, K.D. Maglić, Simultaneous estimation of thermal diffusivity and thermal contact resistance of thin solid films and coatings using the two-dimensional flash method, *Int. J. Thermophys.* 24 (3) (2003) 799–819.
- [11] M.N. Özisik, *Boundary Value Problems of Heat Conduction*, International Textbook Company, 1968, p. 135.
- [12] C.W. Tittle, Boundary-value problems in composite media: quasi-orthogonal functions, *J. Appl. Phys.* 36 (1965) 1486.
- [13] H.S. Carslaw, J.C. Jaeger, *Conduction of Heat in Solids*, Clarendon Press, Oxford, 1959, pp. 30–32.
- [14] D.A. Watt, Theory of thermal diffusivity by pulse technique, *Br. J. Appl. Phys.* 17 (1966) 231–240.